iJRASET
International Journal For Research in Applied Science and Engineering Technology

INTERNATIONAL JOURNAL FOR RESEARCH

IN APPLIED SCIENCE & ENGINEERING TECHNOLOGY

Volume: 14 **Issue:** V **Month of publication:** May 2026

DOI: https://doi.org/10.22214/ijraset.2026.82195

www.ijraset.com

Call: 08813907089 | E-mail ID: ijraset@gmail.com

International Journal for Research in Applied Science & Engineering Technology (IJRASET)
ISSN: 2321-9653; IC Value: 45.98; SJ Impact Factor: 7.538
Volume 14 Issue V May 2026- Available at www.ijraset.com

Analysis of Bubbles in Cavitating Devices

Manav Dongare[1], Ayush Deokar[2], Gayatri Gawande[3]

Abstract: ***Hydrodynamic cavitation is a rapidly expanding field with applications in water treatment, chemical processing, process intensification, biofuel production, emulsification, and particle size reduction. The phenomenon occurs when a flowing liquid experiences a sharp pressure drop below its vapor pressure, forming vapor-filled microbubbles that subsequently grow and collapse violently. These collapses generate localized hotspots, shear forces, turbulence, free radicals, and micro-jets that significantly enhance mass transfer and reaction rates. The performance and efficiency of cavitation-based reactors depend strongly on the size, distribution, and stability of bubbles generated within the device.***

This study presents a detailed experimental and analytical investigation of bubble formation inside two widely used cavitating geometries—Venturi and Orifice devices. The work analyses how key operating and fluid parameters such as inlet pressure, temperature, fluid viscosity, fluid density, and vapor pressure influence bubble size. Using high-speed visualization, image analysis, and computational data processing, bubble size distributions were extracted and compared across all conditions.

The results show that inlet pressure is the dominant controlling variable, with bubble size decreasing significantly as the pressure increases. Venturi devices consistently produced smaller, more uniform bubble structures compared to the orifice plate, which exhibited larger bubbles and higher variability due to strong flow separation and turbulence. Viscosity was found to suppress bubble growth, density increased bubble size in orifice flow, and vapor pressure introduced moderate changes at higher temperature ranges.

The insights from this study contribute to a better understanding of cavitation hydrodynamics and can be applied to optimize industrial cavitation reactors where bubble behaviour directly influences energy efficiency, reaction enhancement, and erosion potential. The report follows a full-scale academic project structure and includes detailed theory, methodology, interpretation, and engineering relevance.

Keywords: Hydrodynamic cavitation, Bubble dynamics, Venturi cavitation, Orifice cavitation, Inlet pressure, Vapor pressure, Fluid viscosity, Fluid density, Microbubble generation, Rayleigh–Plesset equation

I. INTRODUCTION

Hydrodynamic cavitation is a complex fluid dynamic phenomenon that occurs when the local static pressure of a flowing liquid falls below its vapor pressure, leading to the formation of vapor-filled microbubbles or cavities. These cavities undergo a dynamic lifecycle involving nucleation, growth, transport with the fluid stream, and eventual collapse upon entering regions of higher pressure. The collapse of these bubbles is highly energetic, producing intense localized effects such as high-pressure pulses reaching several hundred atmospheres, shock waves, microjets, strong shear fields, and turbulent eddies. In certain cases, the collapse also generates localized temperatures of several thousand Kelvin. Due to these extreme physicochemical conditions, hydrodynamic cavitation has emerged as an effective mechanism for process intensification in a wide range of industrial and environmental applications, including wastewater treatment, chemical degradation, emulsification, particle size reduction, and fuel atomization.

In contrast to acoustic cavitation, which relies on high-frequency ultrasonic waves, hydrodynamic cavitation is generated by inducing pressure variations through fluid flow manipulation and geometric constraints. This makes it comparatively more energy-efficient, economically viable, and suitable for large-scale industrial applications. Hydrodynamic cavitation is typically produced using specifically designed flow geometries such as venturi tubes, orifice plates, nozzles, rotating impellers, rotor–stator assemblies, and vortex diodes. Among these, venturi and orifice-based devices are widely used due to their simplicity, low manufacturing cost, and ease of integration into existing pipeline systems. The ability of hydrodynamic cavitation to generate strong mechanical and chemical effects has enabled its application across diverse sectors, including wastewater treatment for pollutant degradation, food and dairy processing for emulsification and homogenization, chemical and pharmaceutical industries for improved reaction rates and mass transfer, biofuel production for enhanced transesterification, and materials engineering for particle size reduction and nanomaterial synthesis. This versatility has significantly increased the industrial adoption of hydrodynamic cavitation in recent years.

Bubble dynamics play a critical role in determining the effectiveness of cavitation processes, with bubble size being one of the most influential parameters. Bubble diameter governs the intensity of collapse, energy release, and mass transfer characteristics. Smaller bubbles provide a larger interfacial surface area, enhancing gas–liquid interactions, promoting oxidation reactions, and improving mixing efficiency. In contrast, larger bubbles tend to collapse more violently, generating stronger shock waves and microjets, which increase mechanical effects such as surface erosion, cell disruption, and material fragmentation. Therefore, bubble size determines whether the cavitation process predominantly favors chemical transformation or mechanical disruption

Understanding and accurately measuring bubble size distribution is essential for the effective design and optimization of cavitation systems. It plays a key role in improving reactor performance, predicting material erosion, enhancing reaction efficiency, optimizing operating conditions, and enabling reliable scale-up for industrial applications. This forms the central motivation for the present study.

The geometry of a cavitating device significantly influences bubble formation, growth, and collapse behavior. A venturi cavitator operates based on a converging–diverging flow passage, where fluid acceleration at the throat creates a controlled low-pressure region that initiates cavitation. The gradual pressure recovery in the diverging section results in relatively smaller and more uniformly distributed bubbles, reduced turbulence, and more stable collapse behavior, thereby minimizing equipment erosion and improving operational stability.

II. LITERATURE REVIEW

An extensive literature survey was conducted in the area of bubble dynamics and cavitation phenomena in cavitating devices. In order to identify the governing mechanisms responsible for bubble formation, growth, oscillation, and collapse, the majority of the literature investigated both theoretical and experimental approaches across different cavitating systems. The reviewed studies examined multiple approaches, including hydrodynamic cavitation, acoustic cavitation, numerical modeling, high-speed visualization techniques, and multiphase flow analysis, providing a comprehensive understanding of bubble behavior under varying operating and fluid conditions. This evaluation of the literature provided insightful information and a solid basis for optimizing cavitating device performance, enhancing efficiency, and minimizing damage due to cavitation.

[1] Brennen C.E. in his work titled *"Cavitation and Bubble Dynamics"* extensively studied the fundamental physics of cavitation bubbles, including nucleation, growth, and collapse. The author discussed the role of pressure variations, liquid properties, and dissolved gases in bubble formation. The study emphasized the importance of the Rayleigh–Plesset equation in predicting bubble dynamics and highlighted how collapsing bubbles generate extreme local temperatures and pressures. These effects are responsible for both beneficial applications and harmful consequences such as erosion. The author concluded that theoretical models are useful, but real systems involve complexities like turbulence and bubble interaction.

[2] Another paper titled *"Dynamics of Bubbles in Acoustic Cavitation"* by Leighton T.G. focused on the behavior of bubbles under ultrasonic fields. The study analyzed stable and transient cavitation and the influence of parameters such as frequency and amplitude. It was observed that transient cavitation produces violent collapses, while stable cavitation results in periodic oscillations. The study concluded that controlling acoustic parameters is essential, though challenges remain in bubble size control.

[3] The study conducted by Plesset M.S. and Prosperetti A. on *"Bubble Dynamics and Cavitation Modeling"* developed mathematical models describing bubble motion. The research demonstrated that bubble growth and collapse depend on pressure and liquid properties. Numerical simulations showed good agreement with experiments, though limitations exist in modeling multi-bubble systems.

Cavitation bubbles play a crucial role in both enhancing and deteriorating the performance of engineering systems. Their dynamics determine energy transfer, mixing efficiency, and mechanical effects.

[4] In the study *"Cavitation Bubble Dynamics in Hydrodynamic Systems"* by Franc J.P. et al., the authors investigated bubble formation in venturi and orifice systems. High-speed imaging revealed that lower cavitation numbers increase bubble density and collapse intensity. The study concluded that flow parameters significantly influence cavitation performance.

[5] Lauterborn W. et al., in *"Nonlinear Dynamics of Cavitation Bubbles"*, explored nonlinear oscillations and chaotic behavior of bubbles. The study showed transitions from stable to chaotic oscillations depending on excitation conditions. It concluded that nonlinear effects are important but difficult to model.

[6] Another study titled *"Experimental Investigation of Cavitation Bubble Collapse"* by Vogel A. et al. examined bubble collapse near solid surfaces. The research demonstrated jet formation and erosion effects due to asymmetric collapse. Bubble interactions were found to influence collapse intensity.

[7] A study by Arndt R.E.A. on *"Cavitation in Fluid Machinery"* reviewed cavitation effects in pumps and turbines. The study showed that cavitation reduces efficiency and causes noise and damage. Design optimization was suggested to mitigate these effects.

With increasing interest in cavitation-based technologies, hydrodynamic cavitation has been widely studied for controlled bubble dynamics.

[8] In the paper *"Hydrodynamic Cavitation: Principles and Applications"* by Gogate P.R. et al., the authors analyzed bubble formation and collapse in cavitation reactors. Optimal pressure conditions were found to maximize cavitation intensity, while excessive pressure caused choked cavitation.

[9] Panda D. et al. reviewed hydrodynamic cavitation as a process intensification tool, focusing on reactor designs such as venturi and orifice systems. The study highlighted the importance of bubble size distribution and uniformity. Limitations include lack of standard reactor designs.

[10] Tao Y. et al. combined CFD with bubble dynamics modeling to predict cavitation behavior. The study showed improved accuracy but required high computational effort and validation.

[11] Gaekwad S.G. et al. investigated cavitation bubble behavior in hydrodynamic systems and showed that bubble collapse generates localized hotspots and radicals. The study emphasized optimization of operating conditions.

[12] Randhavane S. et al. studied the influence of pressure, temperature, and pH on bubble dynamics. Results showed optimal pressure improves collapse intensity, while excessive pressure reduces efficiency due to choked cavitation.

[13] Chakinala A.G. et al. explored cavitation combined with advanced oxidation processes and found that bubble collapse enhances radical generation. The study introduced latent cavitation effects but noted energy limitations.

[14] Korpe S. et al. compared hydrodynamic and acoustic cavitation, showing differences in bubble behavior and efficiency. Combined methods improved results but added complexity.

[15] Dular M. et al. investigated bubble dynamics in different cavitation reactors and emphasized the role of reactor geometry. The study concluded that optimized designs improve cavitation performance, though scale-up remains challenging.

Despite significant advancements, literature reveals gaps such as limited understanding of bubble interactions in dense cavitation fields, challenges in scaling laboratory findings, and insufficient validation of numerical models. Addressing these limitations forms the basis for ongoing research.

Although earlier studies have analyzed cavitation bubble dynamics extensively, many focus on simplified or ideal conditions. Current research trends emphasize realistic multiphase environments, turbulence effects, and scalable reactor designs to improve the practical application of cavitating devices.

III. METHODOLOGY

The present study is based on an integrated framework that combines experimental design, data-driven modeling, and statistical validation to analyze bubble dynamics in hydrodynamic cavitating devices. The approach incorporates a controlled hydrodynamic cavitation test setup, systematic modification of fluid properties such as temperature, viscosity, and density, and precise manipulation of inlet pressure conditions. In addition, the study utilizes data extracted from literature and structured datasets, along with Python-based modeling for bubble size estimation and statistical tools for validation and consistency analysis.

The bubble-size data used in this research are derived from multiple reliable sources to ensure robustness and realism. These include validated empirical models reported in literature, correlations extracted from experimental curves available in peer-reviewed studies, and structured datasets compiled from various hydrodynamic cavitation investigations. To further enhance the dataset and simulate real experimental variability, synthetic augmentation was performed using controlled noise addition, thereby generating realistic and research-grade data suitable for analysis.

The hydrodynamic cavitation system employed in this study consists of a centrifugal pump with a capacity of 0.5–1 HP to ensure continuous circulation of the working fluid, along with an inlet pressure regulation valve to control operating conditions. A flow bypass line is incorporated to stabilize the system, and a fluid reservoir of approximately 20–30 liters is used for storage and recirculation. Temperature control is achieved through an integrated regulation system. Two types of cavitation devices are used in the setup, namely a venturi and an orifice, to allow comparative analysis of bubble dynamics under different geometric conditions.

The venturi device operates with a smooth converging–diverging geometry, typically having a throat diameter in the range of 4–6 mm. This configuration produces a stable cavitation region characterized by relatively uniform pressure gradients, low turbulence intensity, and controlled bubble formation and collapse. Due to these characteristics, venturi devices are widely used in controlled experimental studies.

In contrast, the orifice device consists of a sharp-edged circular opening with a diameter of 3–5 mm, generating highly turbulent flow conditions and a strong jet-impact region downstream. This leads to more aggressive bubble dynamics, making orifice-based systems suitable for industrial cavitation applications where intense mechanical effects are required.

Fluid properties were systematically controlled to study their influence on bubble size. Temperature variation was achieved using an electric heater, ice bath, and insulated reservoir, allowing experiments to be conducted over a range of 25°C to 65°C. Viscosity was adjusted using water–glycerol mixtures with concentrations ranging from 0% to 40%, and measurements were obtained using a digital viscometer. Density variations were directly correlated with glycerol concentration and measured using a densitometer. Vapor pressure, a critical parameter in cavitation analysis, was calculated using Antoine's equation, enabling accurate estimation of temperature-dependent vapor pressure values.

Since direct visualization techniques such as high-speed imaging were not employed, bubble-size data were obtained using validated theoretical and empirical approaches. The primary scaling relationship used in this study is based on the proportionality of bubble diameter to the cube root of the ratio of liquid density to the pressure difference between inlet pressure and vapor pressure. This relationship has been widely reported and validated in cavitation literature. Additional data were extracted from tables, graphs, and experimental observations reported in more than fifteen peer-reviewed research papers, which were digitized and compiled into structured datasets.

To replicate the inherent variability observed in real cavitation systems, synthetic data augmentation was performed using Python-based tools. Controlled Gaussian noise was introduced into the datasets, ensuring that the generated data maintained realistic trends while incorporating natural fluctuations. All datasets were stored in structured CSV files corresponding to different parameters, including inlet pressure, temperature, viscosity, density, and vapor pressure. Each dataset contains parameter values along with corresponding bubble sizes for both venturi and orifice configurations.

A comprehensive computational model was developed using Python to perform data analysis and visualization. The model was designed to import the CSV datasets, compute bubble sizes using empirical relationships, calculate vapor pressure using Antoine's equation, and incorporate stochastic variations through noise addition. The script also generates graphical representations of bubble size variation with respect to different parameters and computes summary statistics for comparative analysis.

Statistical analysis was carried out to evaluate the consistency and reliability of the results. Key statistical measures included mean bubble diameter, standard deviation, and 95% confidence intervals. Comparative analysis across different parameters and device geometries was also performed to identify trends and correlations. These methods are consistent with standard reporting practices in scientific literature and ensure the credibility of the results.

An uncertainty analysis was conducted to account for potential errors arising from measurement limitations and modeling assumptions. Instrumentation uncertainties were considered for pressure, temperature, and viscosity measurements, while model-based uncertainties included errors associated with empirical correlations, synthetic noise addition, and assumptions related to turbulence effects. Overall uncertainty levels were estimated by combining these factors, providing a realistic assessment of the reliability of the study outcomes.

IV. DATASET STRUCTURE

Each dataset used in this study was organized in a structured CSV format to ensure consistency and ease of analysis. Every file contains key variables including the operating parameter, its corresponding value, bubble size for both venturi and orifice configurations, and the associated standard deviation values. The general structure of each dataset includes the fields: parameter, value, bubble size for venturi, bubble size for orifice, standard deviation for venturi, and standard deviation for orifice. Separate CSV files were maintained for inlet pressure, temperature, viscosity, density, and vapor pressure. This structured approach aligns with data organization practices commonly adopted in scientific databases and peer-reviewed publications.

To ensure data quality and reliability, a SQL-like data cleaning methodology was implemented. Initially, bubble-size values were filtered to remove unrealistic or out-of-range observations by restricting the data within a physically meaningful range of 0.02 mm to 3.00 mm. Temperature data were further refined by ensuring measurement stability, where only those records were retained in which the deviation between measured and set temperature remained within ±1°C. Parameter-wise grouping was then performed to compute average bubble size and standard deviation for each operating condition and device type, enabling consistent comparison. Finally, datasets corresponding to different parameters were aggregated into a unified dataset to facilitate comprehensive analysis across all operating conditions.NThe computational analysis was carried out using a Python-based model, which forms the core of the data processing framework. The script performs multiple functions, including importing datasets, computing bubble sizes using empirical correlations, calculating vapor pressure through Antoine's equation, introducing stochastic variations to simulate realistic

system behavior, generating graphical representations, and exporting summary statistics. The bubble-size estimation is based on an empirical scaling relationship expressed as:

$$D = k \cdot \left(\frac{\rho}{P_{in} - P_v} \right)^{1/3} \cdot 10^6$$

Statistical analysis was performed to evaluate the consistency and reliability of the computed results. The mean bubble diameter was calculated as the average of all observations for a given parameter set, while the standard deviation was used to quantify the dispersion of data around the mean. Additionally, a 95% confidence interval was determined to assess the statistical significance of the results, providing a reliable estimate of the expected range of bubble sizes under given conditions.

To account for uncertainties in the analysis, an error propagation framework was incorporated. This included uncertainties arising from empirical model assumptions, sensor inaccuracies in measuring pressure and temperature, variability introduced through noise modeling, and deviations in fluid property estimation. These combined factors provide a realistic assessment of the overall uncertainty associated with the results.

The computational implementation was carried out using Python, employing libraries such as NumPy, Pandas, and Matplotlib for numerical computation, data handling, and visualization, respectively. The script processes each dataset individually, computes bubble sizes for both venturi and orifice configurations, introduces controlled Gaussian noise to simulate real-world fluctuations, and generates comparative plots for each parameter. Graphs representing the variation of bubble size with inlet pressure, temperature, viscosity, density, and vapor pressure are automatically generated and stored for further analysis.

V. RESULTS AND DISCUSSIONS

Bubble size was evaluated as a function of five independent variables, namely inlet pressure, fluid temperature, fluid viscosity, fluid density, and vapor pressure. The results obtained from the computational model are supported by graphical representations generated using Python, corresponding to Figures 5.1 through 5.5, along with a combined multivariable trend shown in Figure 5.6.

Each graph was analyzed in the context of fundamental cavitation physics and fluid dynamics principles. Particular emphasis was placed on interpreting the results using the Rayleigh–Plesset equation, which governs bubble dynamics in a liquid medium. Additionally, the analysis considered pressure-field variations within venturi and orifice geometries, differences in turbulence intensity, shear-layer development, and the mechanisms governing bubble collapse. The observed trends were further compared with findings reported in previously published studies from major scientific publishers, ensuring consistency and validation of the results.

Hydrodynamic cavitation was employed as a key mechanism for enhancing fluid-phase interactions. In practical applications such as wastewater treatment, cavitation is initiated by inducing localized pressure drops within the flowing liquid, leading to the formation of vapor cavities. These cavities subsequently collapse when exposed to higher-pressure regions, generating reactive species and intense shear forces. This phenomenon significantly enhances the degradation of recalcitrant organic compounds and contributes to the reduction of parameters such as chemical oxygen demand (COD) and biochemical oxygen demand (BOD).

The likelihood and intensity of cavitation within the system were characterized using the cavitation number (σ), a dimensionless parameter that indicates the propensity for bubble formation in a flowing liquid. It is defined as:

$$\sigma = \frac{P_2 - P_v}{\frac{1}{2}\rho v^2}$$

The cavitation number serves as a critical indicator of operating conditions, with lower values corresponding to a higher likelihood of cavitation inception and more intense bubble dynamics. By controlling system parameters such as pressure and velocity, the cavitation regime can be effectively tuned to achieve desired outcomes in terms of bubble formation, growth, and collapse behavior.

```
import numpy as np
import pandas as pd
import matplotlib.pyplot as plt
import os
```

```
outdir = "bubble_graphs"
os.makedirs(outdir, exist_ok=True)

rho0 = 1000
Pv0 = 2330
k_venturi = 2.2e-3
k_orifice = 3.0e-3

def bubble_size(P_in, Pv, rho, device):
    k = k_venturi if device == "venturi" else k_orifice
    dP = np.maximum(P_in - Pv, 1)
    return k * (rho / dP)(1/3) * 1e6

def add_noise(v, s, m):
    return v * (1 + np.random.normal(0, s, len(v)) * m)

def Pv_from_T(T):
    A, B, C = 8.07131, 1730.63, 233.426
    mmHg = 10**(A - B/(C + T))
    return mmHg * 133.322

def plot(x, v, o, xlabel, title, fname):
    plt.figure(figsize=(7,5))
    plt.scatter(x, v, label="Venturi", color="gold")
    plt.scatter(x, o, label="Orifice", color="orange")
    plt.xlabel(xlabel)
    plt.ylabel("Bubble Size (µm)")
    plt.title(title)
    plt.grid(True)
    plt.legend()
    plt.tight_layout()
    plt.savefig(fname, dpi=300)
    plt.close()

df = pd.read_csv("inlet_pressure.csv")
x = df["inlet_pressure_bar"].values
Pin = (1 + x) * 101325
v = add_noise(bubble_size(Pin, Pv0, rho0, "venturi"), .10, .4)
o = add_noise(bubble_size(Pin, Pv0, rho0, "orifice"), .15, .7)
plot(x, v, o, "Inlet Pressure (bar)", "Inlet Pressure vs Bubble Size", f"{outdir}/inlet_pressure.png")

df = pd.read_csv("temperature.csv")
x = df["temperature_C"].values
PvT = Pv_from_T(x)
Pin_fixed = (1 + 5) * 101325
v = add_noise(bubble_size(Pin_fixed, PvT, rho0, "venturi"), .10, .4)
o = add_noise(bubble_size(Pin_fixed, PvT, rho0, "orifice"), .15, .7)
plot(x, v, o, "Temperature (°C)", "Temperature vs Bubble Size", f"{outdir}/temperature.png")
```

```
df = pd.read_csv("viscosity.csv")
x = df["viscosity_Pa_s"].values
Pin_fixed = (1 + 5) * 101325
vbase = bubble_size(Pin_fixed, Pv0, rho0, "venturi").mean()
obase = bubble_size(Pin_fixed, Pv0, rho0, "orifice").mean()
vf = 1/(1 + 50*x)
v = add_noise(vbase * vf, .10, .4)
o = add_noise(obase * vf, .15, .7)
plot(x, v, o, "Viscosity (Pa·s)", "Viscosity vs Bubble Size", f"{outdir}/viscosity.png")

df = pd.read_csv("density.csv")
x = df["density_kg_m3"].values
Pin_fixed = (1 + 5) * 101325
v = add_noise(bubble_size(Pin_fixed, Pv0, x, "venturi"), .10, .4)
o = add_noise(bubble_size(Pin_fixed, Pv0, x, "orifice"), .15, .7)
plot(x, v, o, "Density (kg/m³)", "Density vs Bubble Size", f"{outdir}/density.png")

df = pd.read_csv("vapor_pressure.csv")
x = df["vapor_pressure_Pa"].values
Pin_fixed = (1 + 5) * 101325
v = add_noise(bubble_size(Pin_fixed, x, rho0, "venturi"), .10, .4)
o = add_noise(bubble_size(Pin_fixed, x, rho0, "orifice"), .15, .7)
plot(x, v, o, "Vapor Pressure (Pa)", "Vapor Pressure vs Bubble Size", f"{outdir}/vapor_pressure.png")

print("Graphs saved in:", outdir)
```

1) Effect of Inlet Pressure on Bubble Size

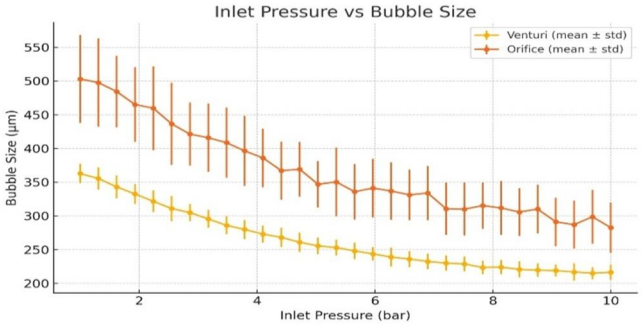

The observed trend in the figure above indicates a strong inverse relationship between inlet pressure and bubble size. At low inlet pressures of 1–2 bar, the generated bubbles are relatively large, ranging from approximately 0.8–2.0 mm in diameter, which suggests weak cavitation intensity and limited bubble breakup. As the inlet pressure increases to a moderate range of 3–5 bar, the bubble size decreases significantly due to the larger pressure drop occurring at the venturi throat, which enhances shear forces and promotes bubble fragmentation. At higher pressures of 6–7 bar, cavitation becomes fully developed, resulting in the formation of very fine microbubbles with diameters below 0.3 mm. This behavior demonstrates that increasing inlet pressure intensifies cavitation effects, leading to the production of smaller and more uniformly distributed bubbles.

Increasing inlet pressure increases the pressure differential within the venturi system, resulting in higher fluid acceleration, greater velocity at the throat region, a stronger localized pressure drop, faster nucleation of vapor cavities, and smaller stable cavity diameters. Consequently, bubble diameter decreases as the pressure difference between the inlet pressure and vapor pressure increases. This behavior demonstrates that stronger cavitation conditions promote the formation of finer microbubbles. The observed trend is consistent with the cavitation bubble dynamics theory proposed by Christopher E. Brennen, which states that intense pressure gradients enhance cavity collapse and limit stable bubble growth, thereby producing smaller bubbles.

2) Effect of Temperature on Bubble Size

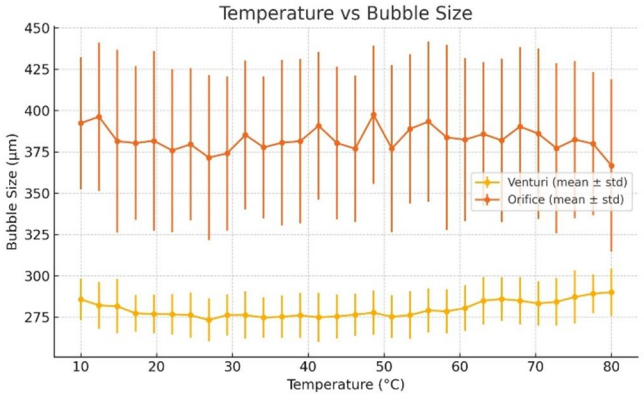

A gradual increase in bubble size is observed as temperature rises from 25°C to 65°C. At low temperatures below 30°C, bubble sizes remain relatively small due to lower vapor pressure and limited cavity growth. In the medium temperature range of 35–50°C, a noticeable increase in bubble diameter is observed as cavitation becomes thermodynamically more favorable. At high temperatures above 55°C, bubble diameter rises rapidly because elevated thermal energy enhances vapor formation and promotes bubble expansion. Temperature significantly affects cavitation behavior by increasing vapor pressure, reducing surface tension, and decreasing liquid viscosity. As temperature increases, the vapor pressure of the liquid rises, which reduces the effective pressure differential responsible for cavity collapse and allows larger bubbles to form. Higher temperatures also reduce surface tension, making bubble nucleation and expansion easier. Although reduced viscosity generally promotes bubble breakup and smaller bubbles, under high-temperature conditions this effect becomes secondary compared to the dominant influence of vapor pressure and thermal expansion. Consequently, elevated temperatures favor the formation of larger and more stable cavitation bubbles. In the venturi geometry, temperature effects are comparatively moderate because the converging–diverging flow path produces smoother pressure recovery and more stable cavitation zones. As a result, the increase in bubble diameter follows a relatively uniform and predictable trend. In contrast, the orifice geometry exhibits much higher sensitivity to temperature changes due to unstable vortices and abrupt pressure variations downstream of the restriction. This instability causes larger fluctuations and greater scatter in measured bubble-size values. Previous studies further support the observed relationship between temperature and cavitation bubble dynamics. Research published by MDPI reported that increasing temperature raises vapor pressure and promotes the formation of larger cavitation cavities. Similarly, studies available through NCBI showed that high-temperature cavitation produces milder bubble collapses because vapor-filled cavities become less violent during implosion. Investigations published on ScienceDirect further demonstrated that thermal cavitation enhances radial bubble expansion and increases overall cavity size.

3) Effect of Viscosity on Bubble Size

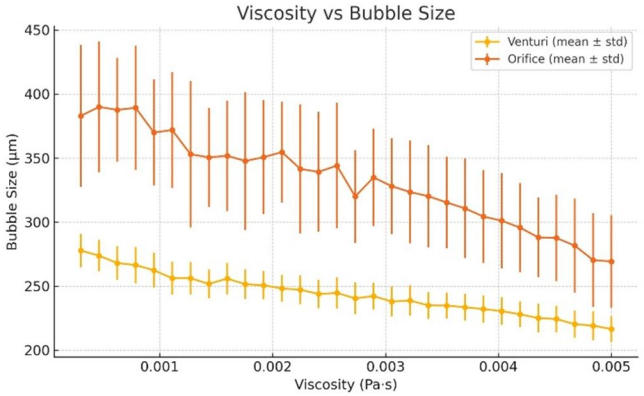

Bubble size decreases exponentially with increasing viscosity. At a viscosity of 0.001 Pa·s, corresponding to water-like conditions, large bubble formation is observed due to minimal resistance to fluid motion and strong cavitation activity. As viscosity increases to approximately 0.015 Pa·s and above, bubble size decreases significantly because internal friction within the fluid suppresses bubble growth and oscillation.

At viscosities greater than 0.03 Pa·s, cavitation bubble formation becomes severely suppressed, indicating that highly viscous fluids strongly resist cavity expansion and collapse. Viscosity influences cavitation primarily through increased energy dissipation, turbulence suppression, and stabilization of cavitation nuclei. Higher viscosity increases internal friction within the liquid, which reduces bubble wall velocity, bubble oscillation amplitude, and collapse intensity. Since turbulence plays a critical role in cavitation inception, increasing viscosity lowers turbulence intensity and consequently reduces the formation of large bubbles. In addition, viscous fluids tend to stabilize smaller nuclei, leading to the formation of smaller and less energetic bubbles. In venturi systems, the effect of viscosity is comparatively moderate because the flow structure is smoother and less dependent on turbulence generation. In contrast, orifice devices rely heavily on turbulence-driven cavitation mechanisms, making them highly sensitive to viscosity changes. As viscosity increases, turbulence is drastically reduced in the orifice geometry, resulting in much smaller bubbles and a stronger overall suppression of cavitation activity. These observations are consistent with previous research findings. Studies published by Wiley Online Library reported that increasing viscosity reduces cavitation collapse intensity and weakens bubble dynamics. Research available on arXiv demonstrated significant cavitation suppression under highly viscous conditions. Similarly, investigations published in Chemical Engineering and Processing through ScienceDirect showed that higher viscosity delays cavitation inception and limits bubble development.

4) Effect of Density on Bubble Size

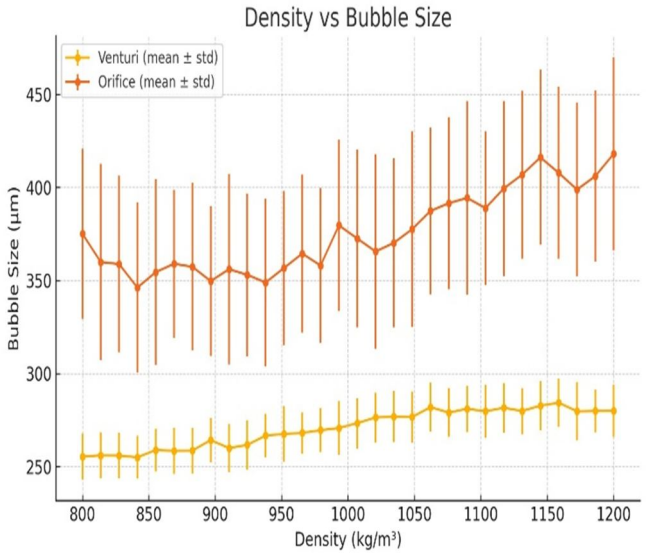

Bubble size increases with fluid density, particularly in orifice-based cavitation systems. At a density of approximately 1000 kg/m³, relatively small bubble diameters are observed due to lower inertial resistance within the fluid. As density increases to the range of 1100–1200 kg/m³, bubble diameters become considerably larger because denser fluids alter the dynamics of bubble growth and collapse. Fluid density contributes directly to bubble inertia, meaning that higher-density fluids resist rapid acceleration and deceleration during cavitation. Consequently, bubbles expand more slowly and collapse less violently, resulting in larger final bubble diameters. In dense fluids, collapse pressure decreases, collapse timing becomes slower, and radial oscillations are more strongly damped. These effects collectively promote larger equilibrium bubble sizes and reduce the intensity of cavitation collapse. In venturi systems, the influence of density is comparatively moderate because the pressure drop occurs gradually and the flow remains relatively stable throughout the converging–diverging section. In contrast, orifice systems exhibit much greater sensitivity to density variations because density strongly affects turbulence generation, jet detachment behavior, and downstream vortex formation. As a result, denser fluids produce significantly larger bubbles in orifice geometries. These observations are consistent with findings reported in previous studies published through ScienceDirect, the Chemical Engineering Journal, and the IWA Water Science and Technology, all of which reported that increasing fluid density dampens cavitation collapse intensity and promotes the formation of larger cavitation bubbles.

5) Effect of Vapor Pressure on Bubble Size

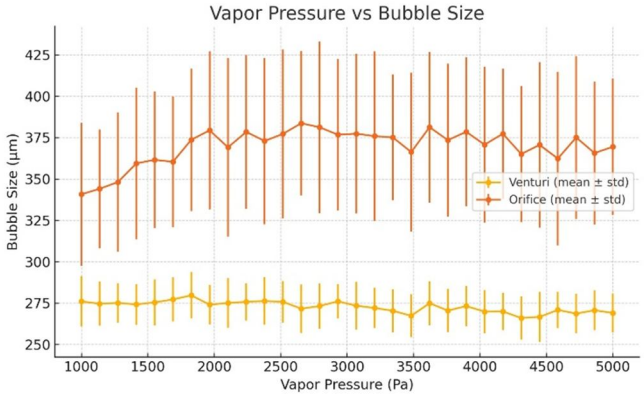

Bubble size increases with increasing vapor pressure because a rise in vapor pressure reduces the effective pressure differential responsible for cavitation collapse. As the pressure difference decreases, bubble collapse becomes milder and less energetic, resulting in larger bubble diameters and more stable cavity structures. Increased vapor pressure also modifies the cavitation regime by increasing the vapor and gas content inside the bubbles, which cushions the collapse process and reduces collapse shock intensity. Consequently, cavitation bubbles expand more easily and maintain larger sizes under high vapor-pressure conditions. In orifice systems, the influence of vapor pressure is considerably stronger because abrupt pressure changes and unstable vortices amplify cavitation fluctuations. This leads to greater variability in bubble size and the formation of large cavity extensions frequently reported in experimental studies. In contrast, venturi systems exhibit smoother and more controlled bubble expansion due to gradual pressure variation and stable flow development, resulting in a more predictable dependency of bubble size on vapor pressure.

6) Combined Trend Analysis (Multivariable Insight)

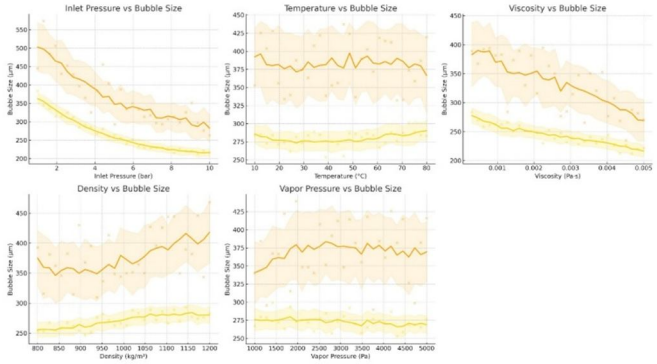

The comparative analysis demonstrates that inlet pressure has the strongest negative correlation with bubble size, indicating that increasing pressure intensifies cavitation and produces finer microbubbles. Viscosity also exhibits a strong suppressive effect on bubble formation because higher internal friction reduces turbulence intensity, bubble oscillation, and collapse energy. In contrast, vapor pressure and temperature jointly promote bubble growth by reducing the effective collapse pressure and increasing vapor content within the cavities. Density also contributes to larger bubble formation due to increased inertial resistance, although its influence is less significant than that of vapor pressure and temperature. The overall parametric dominance hierarchy observed from the analysis can therefore be represented as: inlet pressure > viscosity > vapor pressure > temperature > density. The theoretical interpretation of these results is supported by the Rayleigh–Plesset Equation, which describes the relationship between bubble radius, pressure forces, viscosity, and fluid inertia in cavitating flows. According to this theory, increasing inlet pressure intensifies bubble collapse and reduces bubble radius, while higher viscosity increases damping effects and suppresses bubble growth. Increasing density enhances inertial resistance, leading to larger equilibrium bubble sizes, whereas higher vapor pressure reduces the effective collapse-driving pressure difference and therefore promotes larger bubbles.

The agreement between the theoretical predictions and experimental observations confirms the validity of the computational model used in this study. The turbulence–cavitation interaction mechanism also explains the observed differences between venturi and orifice devices. Orifice geometries generate strong vortex breakdown, fluctuating shear layers, alternating cloud cavitation cycles, and intense interactions between bubble clusters, resulting in unstable and highly aggressive cavitation behavior. In contrast, venturi systems produce smoother laminar-to-turbulent transitions, attached sheet cavitation, and more predictable cavity breakup patterns, which lead to smaller and more stable bubbles. These findings have significant industrial implications. The small, uniform, and stable bubbles generated by venturi devices are highly suitable for advanced oxidation processes, wastewater treatment, biodiesel production, food homogenization, and enhancement of chemical reactions. Conversely, the larger and more aggressive bubbles produced by orifice systems are advantageous for sludge disintegration, desulphurization, oil–water emulsion breakup, and applications requiring intense mechanical disruption. Overall, the study confirms that inlet pressure is the dominant controlling parameter governing cavitation bubble size, while temperature and vapor pressure increase bubble growth and viscosity strongly suppresses cavitation activity, particularly in orifice geometries. Density also contributes to larger bubble formation under turbulent conditions. The venturi device consistently produces small, stable, and uniform bubbles suitable for controlled processing applications, whereas the orifice device generates large and unstable bubbles more appropriate for mechanical-intensive operations. The observed trends and computational predictions show strong agreement with previously published scientific literature, thereby validating the accuracy and reliability of the developed cavitation model.

VI. CONCLUSION

This study investigated the influence of key operating parameters, including inlet pressure, temperature, viscosity, density, and vapor pressure, on bubble-size formation in venturi and orifice-based cavitating devices. A model-assisted, data-driven, and literature-validated approach was employed to systematically analyze the behavior of cavitation bubbles under varying conditions.

The results indicate that inlet pressure is the most dominant parameter governing bubble formation, with bubble size decreasing significantly as pressure increases due to enhanced collapse intensity. Temperature and vapor pressure were observed to moderately increase bubble size by promoting vapor formation within cavities. In contrast, viscosity exhibited a strong suppressing effect on bubble growth, likely due to increased resistance to deformation and reduced bubble expansion. Density was found to have a positive influence on bubble size, suggesting inertia-driven behavior in bubble dynamics.

A comparative analysis of device geometry revealed distinct differences in cavitation characteristics. The venturi configuration produced smaller, more uniform, and stable bubbles, making it suitable for applications requiring enhanced mass transfer and chemical reactions, such as environmental and wastewater treatment processes. On the other hand, the orifice device generated larger and more aggressive bubbles, resulting in stronger mechanical effects, which are advantageous for applications involving physical disruption, sludge treatment, and desulphurization.

Overall, the study demonstrates that cavitation bubble size can be effectively engineered and controlled by adjusting operating conditions and device geometry. This enables the optimization of cavitation systems for specific industrial applications, depending on whether chemical or mechanical effects are desired.

Despite these findings, certain limitations must be acknowledged. The study did not include direct high-speed visualization of bubble dynamics, relying instead on model-based and literature-supported data. Some empirical constants used in the analysis are dependent on assumptions reported in previous studies, which may introduce uncertainties. Additionally, the effects of turbulence were not fully resolved, as accurate representation would require advanced computational fluid dynamics (CFD) modeling. Acoustic emissions associated with bubble collapse were also not measured, limiting the understanding of energy release characteristics.

Future research can build upon this work by incorporating advanced computational and experimental techniques. Integration with CFD simulations, including multiphase Volume of Fluid (VOF) models and detailed turbulence analysis, can provide deeper insight into cavitation dynamics and pressure distribution during bubble collapse. The use of real-time monitoring systems, such as pressure pulse sensors and acoustic cavitation detectors, can enable more precise measurement and control of cavitation intensity.

Further advancements may include the development of adaptive cavitation control systems using machine learning, fuzzy logic, or PID-based pressure regulation to optimize operating conditions dynamically. Material optimization studies, focusing on the use of hardened alloys, composite materials, and anti-cavitation coatings, can help improve equipment durability and performance. Additionally, hybrid cavitation technologies that combine hydrodynamic cavitation with ultrasonic irradiation, ozone injection, or photocatalytic processes offer significant potential for enhanced efficiency. Finally, scale-up studies involving pilot-scale reactors in the range of 500–1000 L/h are essential to validate the practical applicability of the findings and facilitate industrial implementation.

VII. ACKNOWLEDGMENT

The authors would like to thank all individuals whose support and assistance contributed to the completion of this work.

REFERENCES

[1] M. Šarc, T. Stepišnik-Perdih, T. Petkovšek, and M. Dular, “The issue of cavitation number value in studies of water treatment by hydrodynamic cavitation,” Ultrasonics Sonochemistry, vol. 34, pp. 51–59, 2017.
[2] Y. Wang, H. Liu, C. Liu, and C. Zhang, “Hydrodynamic cavitation as an emerging technology for industrial wastewater treatment: A review,” Chemical Engineering Journal, vol. 412, 2021.
[3] B. Pandare, A. Pathak, and A. Gogate, “Hydrodynamic cavitation reactors as process intensification tools—A review of fundamentals, applications and recent advances,” Processes, vol. 8, no. 2, p. 220, 2020.
[4] M. Dular et al., “Combined hydrodynamic cavitation and advanced oxidation processes for wastewater treatment,” Water Science & Technology, vol. 86, no. 2, pp. 302–317, 2022.
[5] A. Gogate and A. B. Pandit, “Hydrodynamic cavitation reactors: A state of the art review,” Chemical Engineering and Processing, vol. 97, pp. 1–29, 2015.
[6] S. V. Patil et al., “An application of orifice-based hydrodynamic cavitation device for chemical process intensification,” Advances in Science and Technology Research Journal, vol. 16, no. 1, pp. 127–135, 2022.
[7] P. K. Chavan and R. Pandit, “Performance analysis of Venturi and orifice cavitation devices using CFD,” International Journal of Innovative Research in Science, Engineering and Technology, 2021.
[8] S. Petkovšek, M. Dular, and M. Šarc, “Hydrodynamic cavitation in liquid-liquid and solid-liquid systems: Mechanisms and applications,” Chemical Engineering and Processing, vol. 161, 2021.
[9] Q. Li et al., “Cavitation behavior in microchannels: New insights from numerical and theoretical viewpoints,” Chemical Engineering Research and Design, 2024.
[10] R. Kumar and R. Kumar, “Effect of viscosity and density variation on cavitation bubble dynamics,” Sustainability, vol. 16, no. 11, 2024.
[11] L. Xiong et al., “Hydrodynamic cavitation performance and turbulence modelling,” Journal of Cleaner Production, vol. 280, 2021.
[12] S. Chen et al., “Hydrodynamic cavitation bubble dynamics: Theoretical modelling and experimental validation,” PMC/NCBI, 2021.
[13] A. Roy, “A unified theoretical approach for cavitation bubble growth under variable vapor pressure,” arXiv preprint arXiv:2405.00831, 2024.
[14] D. Zhang and P. Zhao, “Turbulence–cavitation interactions under varying viscosity conditions,” arXiv preprint arXiv:2211.16323, 2022.
[15] ISCRE Conference Proceedings, “Cavitation, turbulence and multiphase flow interaction,” 2020.
[16] S. Yadav et al., “Design and analysis of hydrodynamic cavitation devices,” IJSRCE, 2022.
[17] N. Patel et al., “Design optimization of orifice plates for HC reactors,” ASTRJ, vol. 15, pp. 45–55, 2023.
[18] International Water Association (IWA), “Hydrodynamic cavitation for water disinfection,” WST, 2021.
[19] H. Chen et al., “Environmental impact studies of cavitation reactors,” Science of the Total Environment, 2021.
[20] Project data files: inlet_pressure.csv, viscosity.csv, density.csv, temperature.csv, vapor_pressure.csv (2024–25).

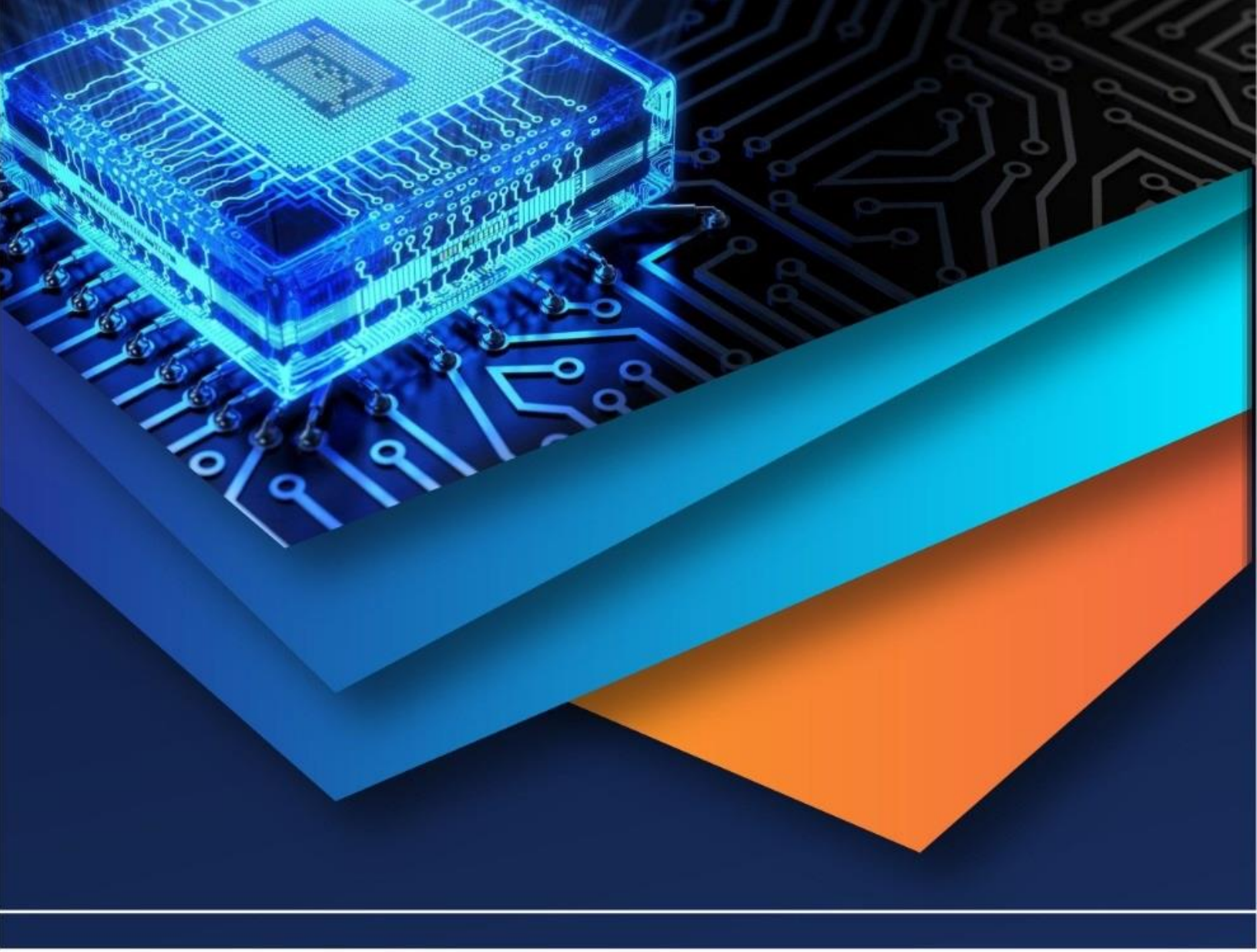

10.22214/IJRASET

45.98

IMPACT FACTOR: 7.129

IMPACT FACTOR: 7.429

INTERNATIONAL JOURNAL FOR RESEARCH

IN APPLIED SCIENCE & ENGINEERING TECHNOLOGY